Spectrochimica Acta, Vol. 36A, pp. 389 to 396

0584-8539/80/0401-0389$02.00/0

Raman spectra and molecular orientation of 7,7′,8,8′-tetracyanoquinodimethane in thin films evaporated on aluminum

M. Ohsawa, W. Kusakari and W. Suëtaka

Laboratory of Interface Science of Metals, Faculty of Engineering, Tohoku University, Sendai 980, Japan

(*Received* 26 *June* 1979)

Abstract—Raman spectra of thin films of 7,7′,8,8′-tetracyanoquinodimethane(TCNQ) evaporated *in vacuo* on aluminum mirrors were measured with external reflection method. Raman intensity was dependent on polarization of the incident laser beam, collection angle of the scattered light, and molecular orientation of the surface species. The optimum conditions for observing Raman spectra of a thin film on metal surface were discussed experimentally and theoretically.

From the collection angle dependence of Raman intensity, it is deduced that the aromatic ring of TCNQ is oriented almost parallel to the metal surface.

1. INTRODUCTION

Raman spectroscopy has recently received attention as a method for *in situ* investigation of the adsorbed molecules on electrodes [1–8] and thin surface films [9–12]. Greenler and Slager [9] have shown theoretically that Raman intensity from a thin film on a metal surface changes remarkably with the incident angle and polarization state of the incident laser beam, and with the collection (or viewing) angle of Raman scattered light. They verified the high sensitivity at the optimum conditions in obtaining Raman spectra of a thin film on a metal surface. Their work was, however, confined to films very thin compared to the wavelength of the laser and Raman scattered lights.

Thicker films are often present, however, on metal surfaces in laboratory and in practical use. When film thickness increases, refraction and phase shift of the lights by the film, which were neglected in their theory, become important and the optimum conditions for observing spectra may change with film thickness. The sensitivity of Raman spectrum is very low compared with u.v.–visible and i.r. spectra, unless a resonance Raman condition is not fulfilled, and observation of spectra of films of weak scatterer is very difficult. It is important, therefore, to determine the optimum conditions for observing Raman spectra of the "thicker" films.

The objects of the present work are (a) to deduce theoretically the optimum conditions for observing Raman spectra of thin films and confirm it experimentally and (b) to show that molecular orientation in a film can be determined from the measurements of angular dependence of Raman intensity.

It is known that 7,7′,8,8′-tetracyanoquinodimethane (TCNQ), evaporated *in vacuo* on cleavage surface of alkali halides, grows epitaxially and the first monolayer adsorbed on the substrates determines the molecular orientation in the thin film crystals [13]. TCNQ may form crystals preferentially oriented also on a metal surface and information about molecular orientation can be used to deduce the metal–adsorbate interaction. For this reason, TCNQ was used in the present paper.

2. EXPERIMENTAL PROCEDURES

Raman spectra were recorded on a Jasco R-300A Raman spectrophotometer equipped with a Spectra-Physics Model 164 Argon ion laser. The optics for the measurements of Raman spectra of surface films is shown in Fig. 1. A film of TCNQ on a sample mirror was excited by the laser beam ($\lambda = 514.5$ nm, 70 mW) polarized parallel ($\parallel$) or perpendicular ($\perp$) to the plane of incidence at the incident angle (ϕ) of 70°. The collection angle of Raman scattered light (ψ) was changed by rotating the sample mirror. At the same time the reflection mirror and prism in the figure were also rotated by the same angle so that the incident plane of the laser coincided with the XZ plane. The polarization of the incident laser beam was adjusted by a half-wave plate. The spectrophotometer was fitted with a polarization scrambler in order to compensate a difference in sensitivity of the spectrometer to the scattered light of different polarizations. Intensity data were based on peak height measurements.

Infrared reflection spectra were recorded on a Jasco IR-G i.r. spectrophotometer equipped with a Jasco PR-41 high sensitivity reflection accessary and a AgCl polarizer.

TCNQ was evaporated *in vacuo* (5×10^{-5} torr) on aluminum mirrors. Film thickness (d) was estimated from the evaporated quantity and the solid angle. Mirrors were prepared by vacuum evaporation of aluminum on glass plates.

3. RESULTS AND DISCUSSIONS

3.1. *Raman spectra*

Figure 2 shows the Raman spectra of TCNQ films of 6, 15 and 50 nm in thickness obtained at $\psi = 0°$ and 60° by using either $\parallel$-polarized (solid curves) or $\perp$-polarized (dashed curves) laser beam. The films were stable against laser illumination during the measurements of the spectra. Frequencies of the bands were almost the same as those of bulk crystal. As can be seen from this figure, band intensities changed with the collection angle and the polarization of the laser beam, and the optimum conditions for obtaining spectra differ from each other depending upon film thickness. In the next section the optimum conditions will be discussed in two cases; (1) $d \ll \lambda$ and (2) $d \approx \lambda$.

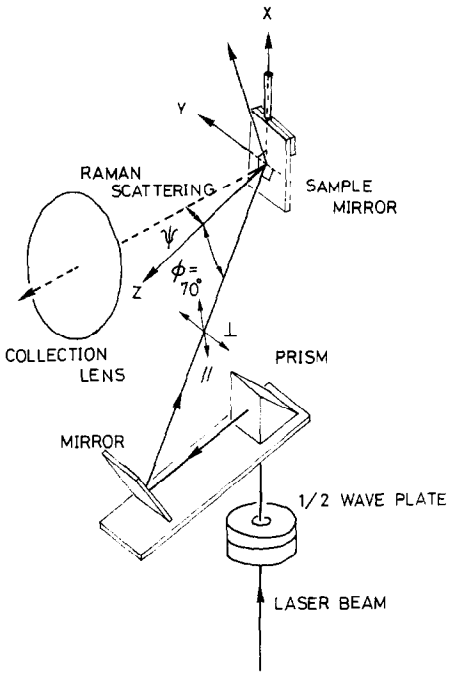

Fig. 1. Optical arrangement used in this work.

3.2. *Very thin films* (d ≪ λ)

Figure 3 shows the collection angle dependence of Raman intensity at 1454 cm^{-1} from a 6 nm thick film for ‖-polarized laser beam. Maximum intensity was obtained at $\psi = 60°$ as being calculated by GREENLER and SLAGER. However the observed angular dependence was slightly different from their calculation (broken line). They treated Raman scattering as a radiation from an oscillating dipole of a molecule on an oxide free metal surface induced by the electric field of the laser beam. According to them, Raman scattering from dipoles oscillating parallel to the surface is remarkably small compared to that from a dipole oscillating normal to the surface and Raman intensity from the former dipoles can be neglected [9]. However Raman intensity measured normal to the surface ($\psi = 0°$) was sizable as shown in this figure. This discrepancy will be discussed below.

The following discussions are based on the GREENLER and SLAGER's treatments of the Raman scattering [9] and the light emission [14] from a thin film on metal surface. Here the Fresnel reflection and transmission coefficients of the interface between two phase j and k are defined, respectively [15]: for ‖-polarization,

$$r_{\|jk} = \frac{\hat{n}_k \cdot \cos\phi_j - \hat{n}_j \cdot \cos\phi_k}{\hat{n}_k \cdot \cos\phi_j + \hat{n}_j \cdot \cos\phi_k},$$

$$t_{\|jk} = \frac{2\hat{n}_j \cdot \cos\phi_j}{\hat{n}_k \cdot \cos\phi_j + \hat{n}_j \cdot \cos\phi_k},$$

and for ⊥ polarization,

$$r_{\perp jk} = \frac{\hat{n}_j \cdot \cos\phi_j - \hat{n}_k \cdot \cos\phi_k}{\hat{n}_j \cdot \cos\phi_j + \hat{n}_k \cdot \cos\phi_k},$$

$$t_{\perp jk} = \frac{2\hat{n}_j \cdot \cos\phi_j}{\hat{n}_j \cdot \cos\phi_j + \hat{n}_k \cdot \cos\phi_k},$$

where ϕ is the angle of incidence or refraction and

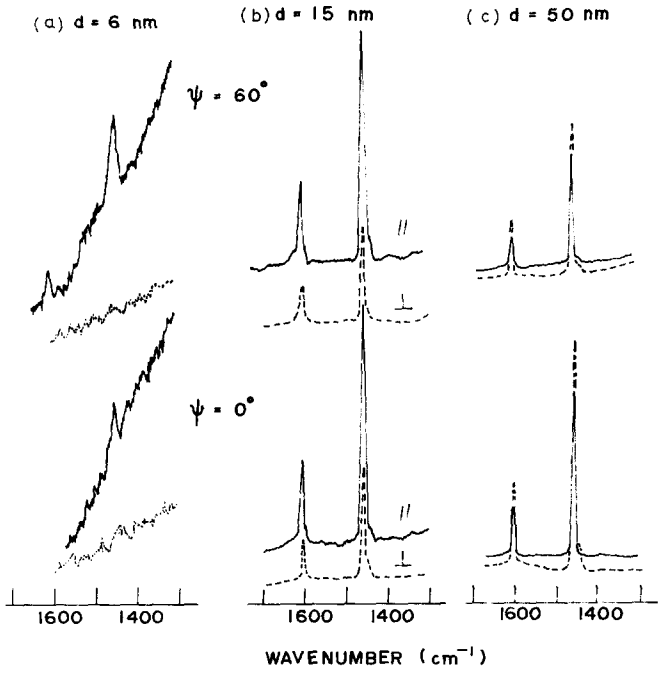

Fig. 2. Raman spectra of TCNQ film evaporated on aluminum mirror obtained with ⊥ and ‖ polarized laser. (λ = 514.5 nm, 70 mW); *d*, film thickness; *ψ*, collection angle of Raman scattered light. Slit width; (a) 500 μm, (b) 350 μm, (c) 120 μm.

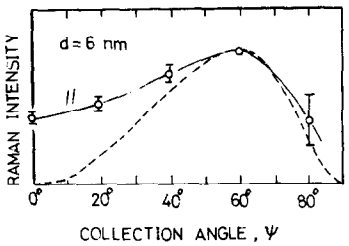

Fig. 3. Collection angle dependence of Raman intensity of the 1454 cm^{-1} band from a TCNQ film in 6 nm thickness. Broken line is calculated according to the GREENLER and SLAGER's theory [9].

$\hat{n}_j(=n_j-ik_j)$ is the complex refractive index of the jth phase.

In the classical picture, Raman scattering can be treated in two processes. The first is the induction of the oscillating dipole of surface species by an excitation beam and the second is the radiation of the energy from the dipole. Since the energy dissipation and refraction of the light in a very thin and non-absorbing film is very small, there is little attenuation of the incident laser and Raman scattered light within the film. An approximation, in which the reflection and refraction of the light at the medium–film interface are neglected, can apply to an extremely thin film on metal surface.

Induction process of the dipole is first considered. When laser beam is specularly reflected from the metal surface, the incident and reflected wave combine to form a standing wave electric field in the incident phase. The electric field strength is the vector sum of the incident and reflected wave [15, 16]. Let us consider the $\perp$-polarized laser beam of unity magnitude. The amplitude of the combined wave at $Z=Z'$ is

$$E_{\perp Y}=1+r_\perp\cdot\exp\left[-i4\pi\left(\frac{Z'}{\lambda}\right)\xi_1\right]$$

where

$$r_\perp=R_\perp^{1/2}\cdot\exp(i\delta_\perp),$$
$$\delta_\perp=\arg(r_\perp)=\tan^{-1}[Im(r_\perp)/Re(r_\perp)]$$

is the phase change on reflection at metal–film interface, and $\xi_1=n_1\cdot\cos\phi$. The coordination system is shown in Fig. 1. The first term shows the contribution from the incident light and second term that of the reflected light. The field strength is expressed as

$$|E_{\perp Y}(Z')|^2=1+R_\perp+2R_\perp^{1/2}\cdot\cos\left[\delta_\perp-4\pi\left(\frac{Z'}{\lambda}\right)\xi_1\right].$$

For $\|$-polarized laser, similarly,

$$|E_{\|Z}(Z')|^2=\sin^2\phi\left\{1+R_\|+2R_\|^{1/2}\cos\left[\delta_\|-4\pi\left(\frac{Z'}{\lambda}\right)\xi_1\right]\right\},$$

$$|E_{\|X}(Z')|^2=\cos^2\phi\left\{1+R_\|-2R_\|^{1/2}\cos\left[\delta_\|-4\pi\left(\frac{Z'}{\lambda}\right)\xi_1\right]\right\}.$$

The induced Raman scattering by these electric fields are expressed for $\|$-polarized laser beam

$$I^0_{\|X}(Z')=\alpha^2_{XX}|E_{\|X}(Z')|^2+\alpha^2_{XZ}|E_{\|Z}(Z')|^2,$$
$$I^0_{\|Y}(Z')=\alpha^2_{YX}|E_{\|X}(Z')|^2+\alpha^2_{YZ}|E_{\|Z}(Z')|^2,$$
$$I^0_{\|Z}(Z')=\alpha^2_{ZX}|E_{\|X}(Z')|^2+\alpha^2_{ZZ}|E_{\|Z}(Z')|^2,$$

and for $\perp$-polarized laser beam

$$I^0_{\perp X}(Z')=\alpha^2_{XY}|E_{\perp Y}(Z')|^2,$$
$$I^0_{\perp Y}(Z')=\alpha^2_{YY}|E_{\perp Y}(Z')|^2,$$
$$I^0_{\perp Z}(Z')=\alpha^2_{ZY}|E_{\perp Y}(Z')|^2,$$

where the subscripts of I, X, Y and Z, represent the oscillating directions of a dipole and α_{XY} etc. are the elements of the Raman tensor based on the space-fixed axes.

We are now at the stage where the radiation process is considered. The amplitude of a light radiated in a ψ direction directly from a dipole A° oscillating along Z axis (Case 1 in Reference [14]) is $A^\circ\sin\psi$. The amplitude of the light reflected from the surface is $A^\circ r_\|\exp[-i4\pi(Z'/\lambda')\xi_1]$. The resultant amplitude after combination is

$$A_Z=A^\circ\cdot\sin\psi\left\{1+r_\|\exp\left[-i4\pi\left(\frac{Z'}{\lambda'}\right)\xi_1\right]\right\}.$$

The observed intensity of the radiation of unity magnitude is, therefore,

$$\varepsilon_Z(Z')=\left(\frac{A_Z}{A^\circ}\right)^2=\sin^2\psi\left\{1+R_\|+2R_\|^{1/2}\cos\left[\delta_\|-4\pi\left(\frac{Z'}{\lambda'}\right)\xi_1\right]\right\}.$$

Similarly the observed intensity of radiation from dipoles oscillating along Y- and X-axis (Cases 2 and 3 in Reference [14]) can be described, respectively,

$$\varepsilon_Y(Z')=\left(\frac{A_Y}{A^\circ}\right)^2=\cos^2\psi\left\{1+R_\|-2R_\|^{1/2}\cos\left[\delta_\|-4\pi\left(\frac{Z'}{\lambda'}\right)\xi_1\right]\right\},$$

$$\varepsilon_X(Z')=\left(\frac{A_X}{A^\circ}\right)^2=1+R_\perp+2R_\perp^{1/2}\cos\left[\delta_\perp-4\pi\left(\frac{Z'}{\lambda'}\right)\xi_1\right].$$

The observed Raman intensity for $\|$ and $\perp$ polarized laser beam is, therefore,

$$I_\|=\int_0^d[I^0_{\|X}(Z)\varepsilon_X(Z)+I^0_{\|Y}(Z)\times\varepsilon_Y(Z)+I^0_{\|Z}(Z)\varepsilon_Z(Z)]\,dZ,$$

$$I_\perp=\int_0^d[I^0_{\perp X}(Z)\varepsilon_X(Z)+I^0_{\perp Y}(Z)\times\varepsilon_Y(Z)+I^0_{\perp Z}(Z)\varepsilon_Z(Z)]\,dZ,$$

respectively.

The next problem to be treated is the explicit expression of the elements α_{XY} etc. in terms of the

elements α_{xy} etc. which are based on the principle polarizability axes of the molecule. We choose to define the xz-plane as the aromatic ring and the z-axis as coincident with the long axis of the molecule. It is well known that TCNQ, evaporated *in vacuo* on cleavage surface of alkali halides, preferentially oriented so that the aromatic ring is almost parallel to the surface [13]. The same molecular orientation is expected also on the metal surface. Let us assume, therefore, an orientation model that the z-axis inclines θ from the Z-axis and the aromatic ring is parallel to the metal surface (XY-plane), as shown in Fig. 4. The validity of this model was verified by using i.r. reflection spectroscopy, as will be mentioned below. There exists a relationship between the tensor components of the above mentioned two coordination systems of the form [17, 18],

$$\alpha_{FF'} = \sum_{gg'} \alpha_{gg'} \Phi_{Fg} \Phi_{F'g'},$$

in which g denotes x, y, z and F denotes X, Y, Z, while Φ_{Fg} is the direction cosine connecting the various pairs of the axes. Since the molecule is considered to be oriented in uniaxial symmetry about Z-axis, $\alpha_{FF'}$ must be averaged over the Eulerian angle ϕ

$$\overline{\alpha^2_{FF'}} = \left(\sum_{gg'} \alpha_{gg'} \Phi_{Fg} \Phi_{f'g'} \right)^2.$$

The 1454 cm^{-1} band of TCNQ is assigned to the in-plane C=C stretching vibrational mode (A_g) [19]. The depolarization ratio of the band was *ca.* 1/3 in acetonitrile solution. This is an indication of the fact that only one diagonal element of the Raman tensor based on the molecule is exceptionally large [20]. Since the C=C stretching mode gives rise to the polarization along the z-axis, it can be considered $\alpha_{zz} \gg \alpha_{xx}$, α_{yy}. Consequently,

$$\overline{\alpha^2_{XX}} = \overline{\alpha^2_{YY}} = \tfrac{3}{8} \sin^4 \theta \cdot \alpha^2_{zz},$$

$$\overline{\alpha^2_{XY}} = \overline{\alpha^2_{YX}} = \tfrac{1}{8} \sin^4 \theta \cdot \alpha^2_{zz},$$

$$\overline{\alpha^2_{XZ}} = \overline{\alpha^2_{ZX}} = \overline{\alpha^2_{YZ}} = \overline{\alpha^2_{ZY}} = \tfrac{1}{2} \sin^2 \theta \cdot \cos^2 \theta \cdot \alpha^2_{zz},$$

$$\overline{\alpha^2_{ZZ}} = \cos^4 \theta \cdot \alpha^2_{zz}.$$

Figure 5 represents the calculated angular dependence of Raman scattering at 1454 cm^{-1} from 6 nm thick film for $\theta = 0$, 45, 73 and 90° and the experimental results. These curves were normalized with

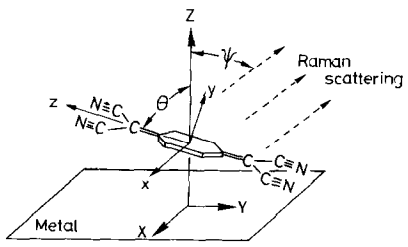

Fig. 4. Orientation model of TCNQ in evaporated film on aluminum.

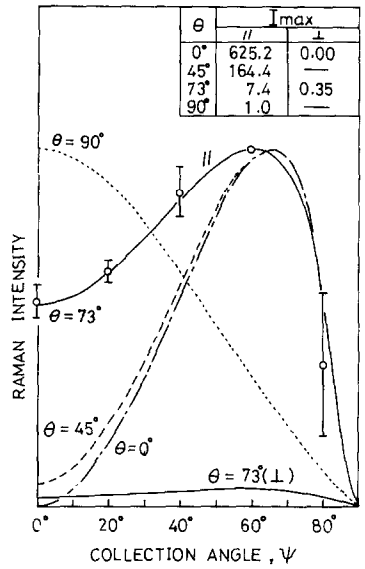

Fig. 5. Calculated and experimental collection angle dependence of Raman intensity of the 1454 cm^{-1} band from a TCNQ film on aluminum in 6 nm thickness of different molecular orientations. Raman intensities are normalized by the maximum values (tabulated in the figure).

their maximum intensities. For the optical constants of the evaporated aluminum mirror for the excitation beam ($\lambda = 514.5$ nm) and Raman scattered light ($\lambda' = 556$ nm) were used the values of $\hat{n} = 0.75$–$5.1i$ and 0.90–$5.5i$, respectively [21]. This figure shows that the angular dependence of Raman scattering changes with molecular orientation and that Raman scattering from a dipole oscillating normal to the surface is observed *ca.* 600-times stronger than that from a dipole oscillating parallel to the surface.

The calculated curve for $\theta = 73°$ and $\parallel$ polarized excitation is in complete agreement with the experimental results except at large collection angles. This discrepancy is mainly because Raman scattered light cannot be collected effectively due to the optical arrangement. The calculated Raman intensity for $\perp$ polarized excitation is one order of magnitude less than that for $\parallel$ polarized excitation. In practice no Raman band was observed by using $\perp$ polarized laser excitation.

Figure 6 shows the angular dependence of Raman scattering at 1454 cm^{-1} from a film of 15 nm in thickness. The observed intensities were normalized at $\psi = 50°$ for $\parallel$ polarized excitation. In this case only slight angle dependence was found except at large angles. The solid curves are calculations for $\theta = 73°$. The calculated intensity for $\perp$ polarized laser excitation is one-third of the experimental result. At the present, the reason for the discrepancy is not clear. However, the presence of a thin oxide layer on aluminum might give rise to the increase in intensity. Since mirror metal was deposited in a low vacuum and exposed to air before film deposition, an oxide film of a few nm in

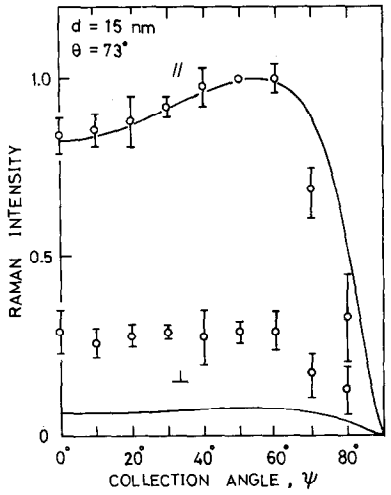

Fig. 6. Collection angle dependence of Raman intensity of the 1454 cm^{-1} band from a TCNQ film in 15 nm thickness for parallel (∥) or perpendicular (⊥) polarized laser. Solid curves are calculations for $\theta = 73°$.

thickness was probably present on the metal surface. Experimental errors in film thickness and Raman intensity measurement might be sizable, resulting in the discrepancy.

3.3. *Thick films* ($d \approx \lambda$)

Figure 7 shows the angular dependence of Raman scattering at 1454 cm^{-1} from a TCNQ film of 50 nm thick. When film was fairly thick, the optimum conditions for observing Raman spectra were different from that in very thin film case. Maximum intensity was brought about at $\psi = 0°$ by using ⊥ polarized laser excitation in this case.

The collection angle and laser polarization dependence of Raman intensity as shown in this figure cannot be explained by the above mentioned

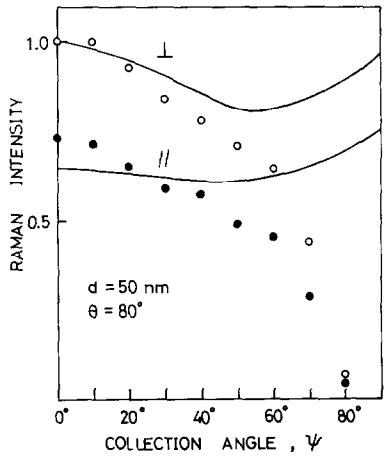

Fig. 7. Collection angle dependence of Raman intensity of the 1454 cm^{-1} band from a TCNQ film in 50 nm thickness for parallel (∥) or perpendicular (⊥) polarized laser. Solid curves are calculations for $\theta = 80°$.

approximation. When film is thick, laser beam and Raman scattered light are refracted by the film. The problem must be treated with three-phase system. The light in the film (phase 2) suffers multiple reflection (Fig. 8) [15]. Upon each reflection at the 1–2 interface the amplitude and phase of the light is changed by a factor r_{21} ($=-r_{12}$). At the 2–3 interface the factor is r_{23}. The total beam at point $Z = Z'$ is the sum of all the lights. For ⊥ polarized laser we have the electric field intensity as

$$E_{\perp 2Y}(Z') = \{t_{\perp 12}\exp[-i\beta(d-Z')] - t_{\perp 12}r_{\perp 12}r_{\perp 123}\exp[-i\beta(3d-z')+\cdots\cdots\} + \{t_{\perp 12}r_{\perp 23}\exp[-i\beta(d+Z')] - t_{\perp 12}r_{\perp 12}r_{\perp 23}^2\exp[-i\beta(3d+z')]+\cdots\cdots\}$$

$$= \frac{t_{\perp 12}\exp[-i\beta(d-Z')]}{1+r_{\perp 12}r_{\perp 23}\exp(-2i\beta d)} + \frac{t_{\perp 12}r_{\perp 23}\exp[-i\beta(d+Z')]}{1+r_{\perp 12}r_{\perp 23}\exp(-2i\beta d)}$$

$$= t_{\perp 12}\exp[-i\beta(d-Z')] \times \frac{[1+r_{\perp 23}\exp(-2i\beta Z')]}{1+r_{\perp 12}r_{\perp 23}\exp(-2i\beta d)},$$

where $\beta = 2n_2\cos\phi_2/\lambda$ and ϕ_2 is given by Snell's law. The terms in the former brace in this equation represent the total lights in the $+Z$ direction and the latter in the $-Z$ direction. Similarly for ∥ polarized laser have

$$E_{\parallel 2x}(Z') = \frac{t_{\parallel 12}\cos\phi_2\exp[-i\beta(d-Z')][1-r_{\parallel 23}\exp(-2i\beta Z')]}{1+r_{\parallel 12}r_{\parallel 23}\exp(-2i\beta d)},$$

$$E_{\parallel 2Z}(Z') = \frac{t_{\parallel 12}\cdot\sin\phi_2\cdot\exp[-i\beta(d-Z')][1-r_{\parallel 23}\exp(-2i\beta Z')]}{1+r_{\parallel 12}r_{\parallel 23}\exp(-2i\beta d)}.$$

The solid curves in Fig. 9 show the calculated intensity of the standing wave electric field in a 50 nm thick film of refractive index $n_2 = 1.45$. The broken curves in this figure show those on a film free aluminum surface. The Z-component of the electric field in the film is very small compared with that in film-free system, owing to the field matching conditions. On the other hand X- and Y- components do not differ so much from each other in these two systems. These results show that Raman intensity from the dipole oscillating perpendicular to the metal surface is not as strong in the $d \approx \lambda$ case, which is different from the $d \ll \lambda$ case.

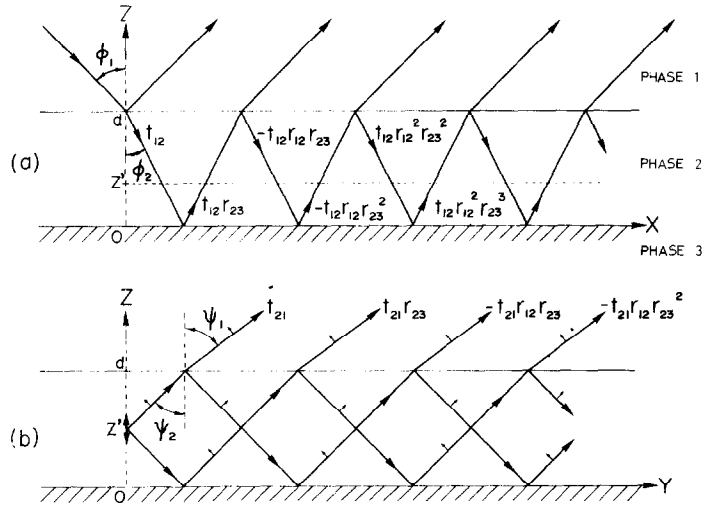

Fig. 8. Multiple reflection of the incident laser beam: (a) Raman scattered light from a dipole oscillating normal to the surface (Case 1, reference [14]; and (b) in a film on metal surface.

Emission process can be treated similarly. Figure 8(b) shows a dipole oscillating along Z-axis (Case 1, reference [14]) for example and we have

$$\frac{A_X(Z')}{A^0} = \frac{t_{\perp 21}\exp[-i\beta(d-Z')][1+r_{\perp 23}\exp(-2i\beta Z')]}{1+r_{\perp 12}r_{\perp 23}\exp(-2i\beta d)},$$

$$\frac{A_Y(Z')}{A^0} = \frac{\cos\psi_2 \cdot t_{\parallel 21}\exp[-i\beta(d-Z')][1-r_{\parallel 23}\exp(-2i\beta Z')]}{1+r_{\parallel 12}r_{\parallel 23}\exp(-2i\beta d)},$$

$$\frac{A_Z(Z')}{A^0} = \frac{\sin\psi_2 \cdot t_{\parallel 21}\exp[-i\beta(d-Z')][1+r_{\parallel 23}\exp(-2i\beta Z')]}{1+r_{\parallel 12}r_{\parallel 23}\exp(-2i\beta d)}.$$

The solid curves in Fig. 7 represent the calculated angular dependence of Raman intensity at 1454 cm^{-1} for $\theta = 80°$ in taking into account of the refraction of the lights by the film. Since the optical constant of the film is unknown, the value $n_2 = 1.45$, usual for organic crystals, was used in the present calculation. The negative deviation of the experimental results from the calculation at high collection angles might be due to the experimental difficulties of collecting Raman scattered light effectively at these angles.

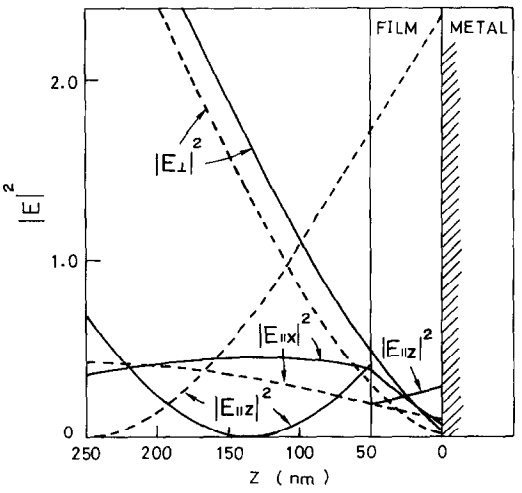

Fig. 9. Electric field intensity on a film-free surface (broken lines) and on a film-covered surface (solid lines). The optical parameters are: $n_1 = 1.0$, $n_2 = 1.45$, $\hat{n}_3 = 0.74-5i$; $d = 50$ nm; $\lambda = 514.5$ nm; $\phi = 70°$.

3.4. *Infrared spectra of TCNQ films*

Infrared reflection spectroscopy is one of the useful methods to investigate the molecular orientation on metal surface. Figure 10 shows the spectra of a TCNQ film in 300 nm thickness obtained by using either of the i.r. radiation polarized parallel ($\parallel$) or perpendicular ($\perp$) to the plane of incidence at the incident angle of 75°. Intensities of the 856 and 437 cm^{-1} band increased markedly in changing polarization from $\perp$ to $\parallel$, while those of the 1543 and 1352 cm^{-1} bands are nearly the same in both the spectra. The former bands are assigned to the out-of-plane CH bending and $C(CN)_2$ wagging vibrations and the latter to the in-plane ring and CH stretching vibrations [19]. According to the theory of reflection spectroscopy [22, 23], the dipole moments of the surface species oscillating normal to the surface interact strongly with the $\parallel$ component of the i.r. radiation, on the other hand dipole moments oscillating parallel to the surface with the $\perp$ component. It is concluded, therefore, that the aromatic ring of TCNQ is nearly parallel to the surface. This result is in agreement with that of Raman studies. Unfortunately, i.r. spectra of films of less than 100 nm in thickness was too poor to provide any information about molecular orientation.

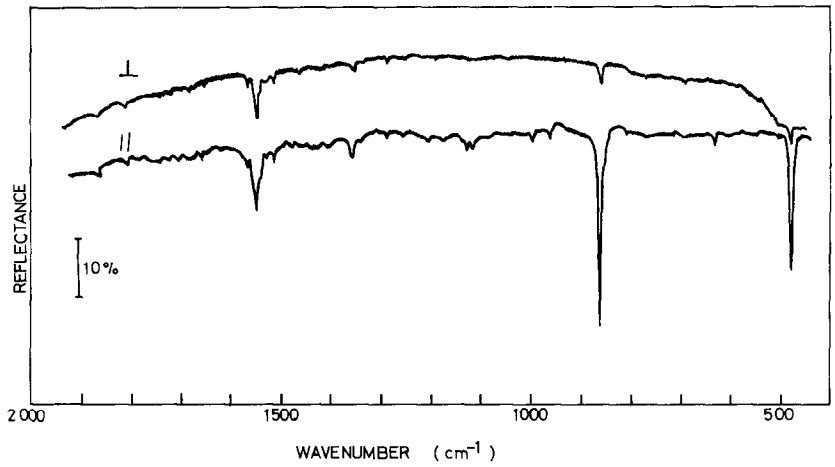

Fig. 10. Infrared reflection spectra of a TCNQ film in 300 nm thickness obtained with parallel (||) or perpendicular (⊥) polarized component of the i.r. radiation.

3.5. *Raman spectra of adsorbed pyridine on silver*

Extremely intense Raman scattering from pyridine adsorbed on silver electrode has been reported [1, 4–8]. This very intense Raman scattering has been considered to come from monolayer or submonolayer adsorbed species. If this were true, maximum intensity should be obtained at a collection angle of *ca.* 60° by using ∥ polarized laser. In our experiments, however, maximum intensity was obtained at a collection angle of 0° by using ⊥ polarized laser and the angular dependence of the Raman intensity was similar to that of fairly thick TCNQ films. Based on the discussion mentioned above, pyridine on silver electrode seems to form a fairly thick layer. In addition our modulation Raman spectroscopic experiments [8] show that only a few tens % of Raman intensity changes by electrode potential modulations. It may be considered, therefore, that not only adsorbed pyridine but also a condensed phase of pyridine are present at the solution–electrode interface. The details of the experiments will be reported shortly.

4. CONCLUSIONS

The optimum conditions for observing Raman spectra of thin films on metal surface was investigated experimentally and theoretically. Intensities of Raman scattering from surface films varied with the laser polarization states, collection angle of the scattered light, and molecular orientations of surface species. When film is very thin compared with the wavelength of the laser ($d \ll \lambda$), maximum sensitivity was obtained by using parallel polarized laser excitation and by collecting Raman scattering at a collection angle of *ca.* 60°, as estimated by Greenler and Slager. As film thickness increased, the influence of the refraction and phase change of the laser and Raman scattered lights by the film becomes important, and the maximum sensitivity was achieved by using perpendicular polarized laser and by collecting Raman light normal to the surface.

By the analysis of the collection angle dependence of Raman scattering, molecular orientation of TCNQ in evaporated films on aluminum were deduced.

Acknowledgement—The laser Raman spectrophotometer employed in the present work was obtained by the financial support of the Mitsubishi Foundation to which thanks are due.

REFERENCES

[1] M. Fleischmann, P. J. Hendra and A. J. McQuillan, *Chem. Phys. Lett.* **26,** 163 (1974).
[2] A. J. McQuillan, P. J. Hendra and M. Fleischmann, *J. Electroanal. Chem.* **65,** 933 (1975).
[3] R. P. Cooney, E. S. Reid, M. Fleischmann and P. J. Hendra, *J. Chem. Soc. Faraday Trans. I* **73,** 1691 (1977).
[4] D. L. Jeanmaire and R. P. van Duyne, *J. Electroanal. Chem.* **84,** 1 (1977).
[5] J. A. Creighton, M. G. Albrecht, R. E. Hester and J. A. D. Matthew, *Chem. Phys. Lett.* **55,** 55 (1978).
[6] B. Pettinger and U. Wenning, *Chem. Phys. Lett.* **56,** 253 (1978).
[7] B. Pettinger, U. Wenning and D. M. Kolb, *Ber. Bunsenges. Phys. Chem.* **82,** 1326 (1978).
[8] W. Suëtaka and M. Ohsawa, *Appl. Surface Sci.* **3,** 118 (1979).
[9] R. G. Greenler and T. L. Slager, *Spectrochim. Acta* **29A,** 193 (1973).
[10] R. N. Zitter, *Surface Sci.* **28,** 335 (1971).
[11] J. A. Cape, L. G. Hale and W. E. Tennant, *Surface Sci.* **62,** 639 (1977).
[12] A. Otto, *Surface Sci.* **75,** L392 (1978).
[13] N. Uyeda, Y. Murata, T. Kobayashi and E. Suito, *J. Crystal Growth* **26,** 267 (1974).
[14] R. G. Greenler, *Surface Sci.* **69,** 647 (1977).
[15] J. A. Johnson and D. W. Peterson, *Surface Sci.* **16,** 217 (1969).

[16] W. N. HANSEN, *J. Opt. Soc. Am.* **58,** 380 (1968).
[17] E. B. WILSON, J. C. DECIUS and P. C. CROSS, *Molecular Vibrations*, p. 285. McGraw-Hill, New York (1955).
[18] T. TAKENAKA and T. NAKANAGA, *J. Phys. Chem.* **80,** 475 (1976).
[19] T. TAKENAKA, *Spectrochim. Acta* **27A,** 1735 (1971).
[20] O. S. MORTENSEN, *Chem. Phys. Lett.* **3,** 4 (1969).
[21] J. M. BENNETT and M. J. BOOTY, *Appl. Optics* **5,** 41 (1966).
[22] S. A. FRANCIS and A. H. ELLISON, *J. Opt. Soc. Am.* **49,** 131 (1959).
[23] R. G. GREENLER, *J. Chem. Phys.* **44,** 310 (1966).